Theoretical and Applied Climatology (2025) 156:208
https://doi.org/10.1007/s00704-025-05437-8

RESEARCH

Investigation of the meteorological and hydrological drought characteristics in yeşilirmak basin, Türkiye

Mehmet Ishak Yuce[1] · Ali Aytek[2] · Musa Esit[3] · Ibrahim Halil Deger[4] · Islam Yasa[5] · Abdulselam Simsek[6] · Fetihhan Ugur[1]

Received: 14 March 2024 / Accepted: 13 March 2025 / Published online: 21 March 2025

Abstract

This research has examined meteorological and hydrological droughts, considering the need for comprehensive studies on drought and its significant damage. This research considers monthly rainfall data from 16 meteorological stations and monthly streamflow data from 12 hydrological gauging stations. This paper aims to conduct a thorough examination of meteorological and hydrological droughts utilizing the standardized precipitation index (SPI) and the standardized streamflow index (SDI) over timescales of 1 (monthly), 3 (seasonal), and 12 (annual) months in the Yeşilırmak basin, Türkiye. The Mann–Kendall (MK) and Spearman Rho (SRHO) are employed at all stations to identify monthly trends, respectively. In addition, Wavelet Transform Coherence (WTC) are performed internal connections between the meteorological and hydrological drought in the basin. Trend test results indicate significant drought trends at 1- and 3-month timescales, while no significant trend is observed at the 12-month timescale. The investigation focuses on understanding the connections between drought conditions observed at hydrological and meteorological stations. The trends are more clearly visible when analyzing data over a 1-month period, compared to analyses covering 3-month or 12-month periods. The SPI and SDI indices show the strongest correlation in the northern part of the basin, while the weakest correlation is observed in the eastern region.

1 Introduction

Drought stands as a considerable natural calamity (Xu et al. 2019) and it impacts the agricultural, ecological, and socioeconomic areas. Due to both climate change and human influences, droughts are occurring more frequently and widely in various regions of the world (Wang et al. 2018; Lai et al. 2019; Esit et al. 2021; Abro et al. 2022). Several researchers have offered a comprehensive overview of the definition of drought, its tracking methods, and recent advancements (Mishra et al. 2010; AghaKouchak et al. 2015; Yuce and Esit 2021; Yildirim and Aksoy 2022). The main classification of drought is into different categories, such as meteorological, agricultural, and hydrological drought, depending on the different forms of water shortages (Mishra et al. 2010). A shortage of surface or groundwater is indicated by a hydrological drought, while insufficient atmospheric and soil water supplies are typically associated with meteorological and agricultural droughts, respectively (Vicente-Serrano et al. 2012a). During a prolonged meteorological drought lasting several months, soil drought typically emerges initially, leading to crop losses, before progressing into an agricultural drought. This prolonged meteorological drought subsequently affects agro-based industries directly. In cases of hydrological drought, response times (duration) are notably slower (Abeysingha et al. 2020; Yaşa and Partal 2024). Given the complexity of drought as a phenomenon, there are several proposed drought indices to determine and track several drought events. The Palmer drought severity index (PDSI), the standardized precipitation index (SPI) (McKee et al. 1993), commonly performed in the USA,

✉ Musa Esit
mesit@adiyaman.edu.tr

1 Civil Engineering Department, Gaziantep University, Gaziantep, Türkiye

2 Civil Engineering Department, Gaziantep Islam Science and Technology University, Gaziantep, Türkiye

3 Civil Engineering Department, Adiyaman University, Adiyaman, Türkiye

4 Civil Engineering Department, Hasan Kalyoncu University, Gaziantep, Türkiye

5 Civil Engineering Department, Ondokuz Mayis University, Samsun, Türkiye

6 Civil Engineering Department, Kirsehir Ahi Evran University, Kirsehir, Türkiye

(Palmer 1965; Alley 1984) and the standardized precipitation evapotranspiration index (SPEI) (Vicente-Serrano et al. 2010) represent the most renowned and widely employed meteorological drought metrics. In addition, Due to their strong link with soil moisture, they have also been used in agricultural droughts (Zambrano et al. 2017). Among all developed indices, SPI is considered the reference for other indices according to the World Meteorological Organization (WMO 2006). Because SPI is calculated for any given location based on its long-term precipitation history over the selected period. Hydrological drought is regarded as the form that is most representative since it assesses streamflow in addition to being able to depict the state of the drought throughout the region (Madadgar and Moradkhani 2014; Wu et al. 2016, 2018). There are several hydrological drought indices available, including the standardized runoff index (SRI) (Shukla and Wood 2008) and the standardized streamflow index (SDI) (Vicente-Serrano et al. 2012a, b). SDI is simple to use and accepts missing data. Additionally, like SPI, several time scales can be considered for drought monitoring. However, relying just on streamflow input can bias the conclusions since it ignores management choices and periods of no flow (Abeysingha et al. 2020). There are many studies in different climates on hydrological drought calculation using the SDI index (Aghelpour et al. 2021; Abbas and Kousar 2021; Simsek 2021; Jamal et al. 2022). Rivera et al., (2017) utilized the SDI to characterize an extreme hydrological drought event in Argentina and found that it effectively captured its evolution and characteristics in the region. Malik et al., (2021) employed the SDI to study hydrological drought at the Kedar and Naula stations situated in the upper Ramganga River catchment in India. Utilizing long-term satellite remote sensing precipitation data, Lai et al., (2019) employed the SDI to investigate hydrological drought in the Beijiang River basin of China. Their study demonstrated that the SDI was highly applicable for modeling and quantitatively analyzing hydrological drought in the Beijiang River basin. Peña-Gallardo et al., (2019) computed the SDI for every basin across the contiguous United States, revealing the intricate connections between meteorological and hydrological drought timescales.

Two drought indices, namely the Streamflow Drought Index (SDI) and the Standardized Precipitation Index (SPI), have been employed to assess the connection between hydrological and meteorological droughts. Hydrometeorological droughts are complex hazards resulting from significant water availability deviations from long-term average conditions (Meresa et al. 2023). Furthermore, the genesis and propagation of hydrometeorological droughts are dictated by a complex interplay of hydrological processes acting across diverse spatial scales. These processes encompass precipitation regimes, evapotranspiration rates, overland flow dynamics, soil moisture content, groundwater storage capacity, and discharge characteristics (Ganguli et al. 2022). A comprehensive analysis is crucial to unravel the relationships between various drought types. This knowledge is essential to predict how climate change might alter drought characteristics, including magnitude, frequency, duration, and propagation (Satoh et al. 2022). For example, Tijdeman et al., (2018) illustrated the interaction between several hydrologic and meteorological drought indices for various watersheds in the contiguous United States considering both human and natural factors. Cheraghalizadeh et al., (2018) assessed the correlation between hydrological and meteorological droughts downstream and upstream of the Kasilian basin by employing a copula-based joint meteorological-hydrological drought index model. The presence of a time lag between meteorological and hydrological droughts is pivotal for efficient drought management., according to some researchers who explored the connection between hydrological and meteorological droughts using various methodologies (Wu et al. 2016; Sattar et al. 2019; Abbas et al. 2021). Tokarczyk & Szalińska, (2014) evaluated the SDI and SPI in two Polish watersheds. The findings demonstrated that meteorological and hydrological drought were frequently connected. Ahmadalipour et al., (2017) examined the Willamette River basin's hydrological and meteorological drought in the Northwest Pacific basin. To assess the impacts of climate change, they utilized the atmospheric global circulation model of the GCMs alongside the CMIP5 downscaling model. For the simulation of rainfall-runoff, they used the PRMS distributed hydrological model. Based on the results, it was observed that while a hydrological drought requires a significantly longer time to develop and subsequently recover, a meteorological drought can commence and conclude more quickly.

While earlier studies on the Yeşilırmak Basin only addressed one type of drought such as meteorological (Boustani and Ulke 2020; Cemek et al. 2022), This research investigates the relationship between meteorological and hydrological drought in the Yeşilırmak Basin, using drought indices as indicators. While the Yeşilırmak Basin is one of Turkey's most important, it has lacked extensive study on hydrological drought. We utilize monthly streamflow data from 12 hydrological gauging stations and monthly precipitation data from 16 meteorological stations to address this gap. This study examines the relationship between hydrological and meteorological drought by analyzing SPI and SDI indices at monthly, seasonal, and annual timescales (1, 3, and 12 months respectively). We use Wavelet Transform Coherence (WTC) to assess the correlation between these drought indices, while temporal trends in drought conditions are evaluated using Spearman Rho (SRHO) and Mann–Kendall (MK) tests on a monthly basis. This study contributes in several ways. Firstly, it offers insights into the mechanisms driving drought development and progression

in the Yeşilırmak basin, laying the groundwork for a drought early warning system. Secondly, it enhances understanding of the water cycle in the Yeşilırmak basin, facilitating better drought monitoring and prevention, and enhancing the utilization, management, and planning of water resources. By elucidating the hydrometeorological drought characteristics of the Yeşilırmak basin, a critical water resource for Turkey, this study offers valuable insights for policymakers, meteorologists, and agricultural researchers.

2 Materials and methods

2.1 Study area and data

The Yeşilırmak Basin has a total area of about 3,873,280 hectares. The basin's area as a percentage of Turkey's land is 5%. Yeşilırmak Basin has a very large area located within the borders of the Black Sea and Central Anatolia regions. The basin is bounded by the water section line passing through the peaks of Canik, Gümüşhane, Giresun, Köse, Çimen, Pulur, Kızıldağ, Yıldız, Tekeli, Çamlıbel, Karababa, Akdağlar, Kunduz, İnegöl Mountain and the Black Sea. While most of the basin is in the Central Black Sea Region, it also has borders in the Eastern Black Sea Region, Upper Kızılırmak Region, and Middle Kızılırmak Region. The basin, influenced by the Black Sea climate, experiences an annual average precipitation of 528 mm/m^2, with an average annual flow of 6.10 km^3. The annual average temperature stands at 12 °C, while the average basin yield is 5.11 l/s/km^2 (KatiPoğlu et al. 2022). Furthermore, the basin holds significant importance for activities such as generation, hydroelectricity, drinking water supply, irrigation, and industrial usage. Assessing the drought status of the basin is crucial for devising actionable plans to address potential challenges (Boustani and Ulke 2020). Data within and surrounding the Yeşilırmak basin are utilized (see Fig. 1). Monthly rainfall data are acquired from the Turkish State Meteorological Service, while streamflow data are collected from the State Hydraulic Works. Table 1 provides geographical details and recording periods of the hydrological and meteorological stations involved in this investigation.

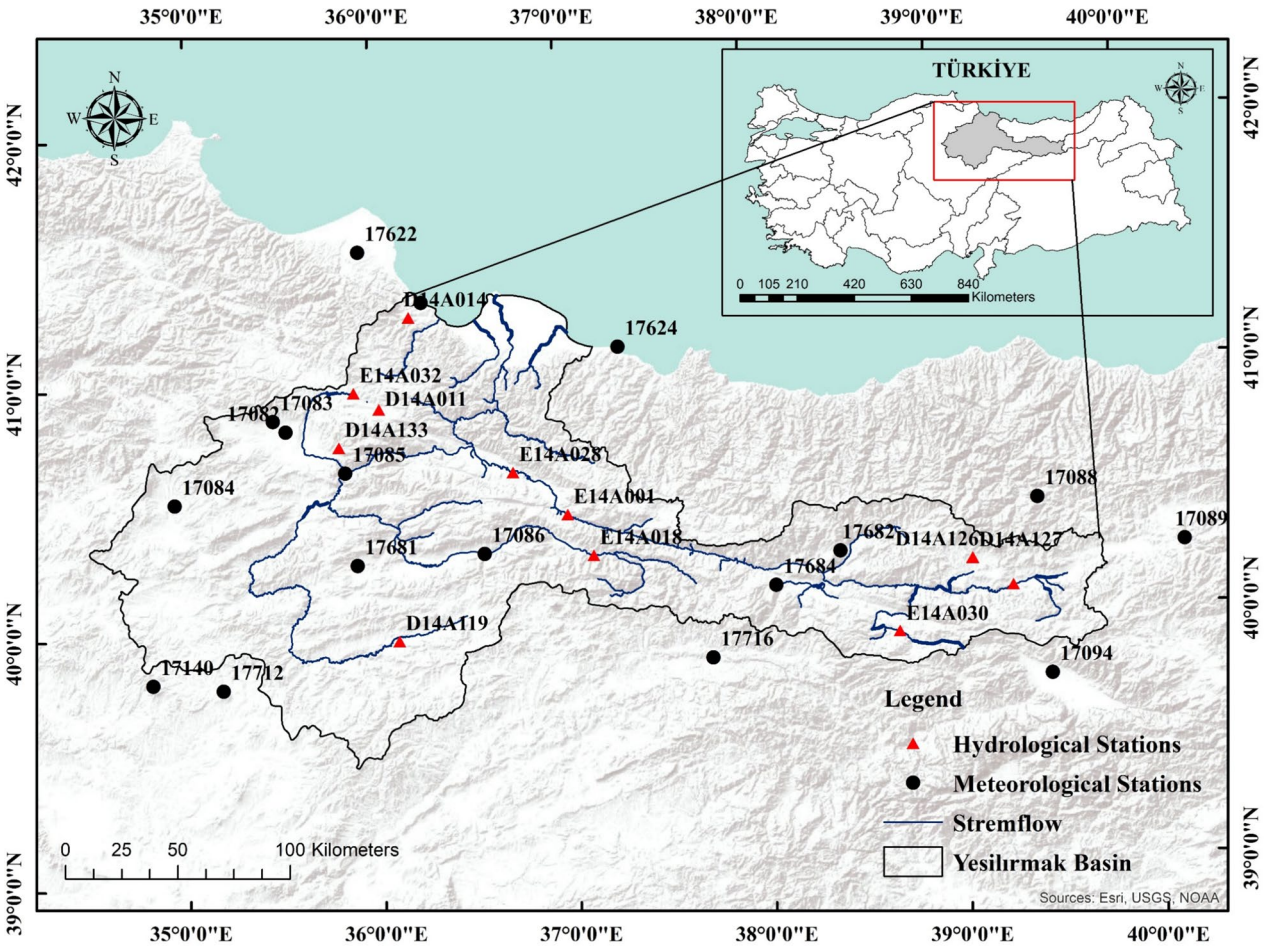

Fig. 1 The locations of stations in the Yeşilırmak Basin

Table 1 The wetness/dryness categories based on SPI and SDI values

Category	Criterion
Non-Drought	SPI, SDI ≥ 0.0
Mild drought	−1.0 ≥ SPI, SDI < 0.0
Moderate drought	−1.5 ≥ SPI, SDI < −1
Severe drought	−2.0 ≥ SPI, SDI < −1.5
Extreme drought	SPI, SDI < −2.0

2.2 Meteorological and hydrological drought assessment

The standardized precipitation index (SPI) approach has gained popularity as a tool for assessing droughts under a variety of climatic conditions and over several time scales (McKee et al. 1993). The Standardized Precipitation Index (SPI) has gained widespread popularity and extensive usage in climate research literature due to several compelling factors. Firstly, SPI is characterized by its simplicity and ease of use. Its calculation relies solely on readily available precipitation data, making it accessible to researchers across various domains and regions. Secondly, the index offers a standardized approach, enabling the comparison of precipitation anomalies across different locations and time scales. This standardization proves invaluable for analyzing drought events in regions exhibiting diverse precipitation patterns(Anshuka et al. 2019; Esit et al. 2023a). In addition, The World Meteorological Organization (WMO) recommends SPI for global use due to its ability to indicate relative precipitation amounts over specific periods (Pei et al. 2020; Yalçın et al. 2023). A gamma distribution is utilized to initially characterize the instanbility of precipitation totals before being transformed into a normal distribution. It is described as follows by the gamma distribution's frequency or probability density function:

$$g(x) = \frac{1}{\beta^{a}\Gamma(\alpha)}x^{a-1}e - \frac{x}{\beta} for x > 0 \quad (1)$$

where x is the amount of precipitation, α and β note as the shape and scale parameters, respectively, and Γ (a) is the gamma function. Maximum Likelihood Estimation (MLE) can be used to calculate these parameters:

$$\alpha = \frac{1}{4A}\left[1 + \sqrt{1 + \frac{4A}{3}}\right], \beta = \frac{\bar{x}}{\alpha}, A = (\bar{x}) - \frac{\sum \ln(x)}{n} \quad (2)$$

where n shows the number of observations.

Using the chosen parameters, the cumulative probability of a precipitation event that has been recorded for the specified month and time frame for the location in question is then calculated. The gamma distribution G(x) could not be established for monthly precipitation of zero magnitudes (x = 0), hence the cumulative probability becomes:

$$H(x)=q+(1-q)G(x) \quad (3)$$

where The probability of an event of zero magnitude rainfall is denoted by q, while the cumulative probability of the incomplete gamma function is represented by G(x). (Boudad et al. 2018). According to McKee et al., (1993), the basin is classified into wetness and dryness groups based on SPI (Table 2).

"Hydrological drought" describes insufficient amounts of groundwater and water, including river flows, groundwater levels, and lake and reservoir water. The level of the water in rivers, reservoirs, lakes, and groundwater is used to assess a hydrological drought (Tabari et al. 2013; Akbari et al. 2015; Malik et al. 2019). This study employs a similar premise to the SPI, namely the standardized streamflow index (SDI) (Nalbantis and Tsakiris 2009), to examine the hydrological drought. The flow data given in Eq. 4 is represented as $Q_{a,b}$, where k stands for the reference period, "a" for the hydrological year, and "b" for the month in a water year. Equation 4 describes how the SDI technique evaluates the cumulative flow volume (Nalbantis 2008).

$$V_{a,k} = \sum_{j=1}^{3k} Q_{a,b} a = 1, 2, \ldots b = 1, 2, \ldots, 12k = 1, 2, 3, 4 \quad (4)$$

In Eqs. 4 and 5, the computations have been performed using the following values: k = 1 for the October-December period, k = 2 for the October–March period, k = 3 for the October-June period, and k = 4 for the October-September period. Based on the cumulative discharge volumes, the following are the SDI values for each k period of a hydrological year:

Table 2 The relationship between hydrological and meteorological stations in the Yeşilırmak basin at different time frames

Time Scale	D14A014-17030	D14A133-17,085	E14A018-17086	E14A022-17088	E14A022-17094	E14A001-17086	D14A119-17,681
1	0.40	0.35	0.30	0.18	0.19	0.13	0.20
3	0.48	0.40	0.38	0.28	0.27	0.21	0.33
12	0.49	0.54	0.53	0.45	0.45	0.35	0.58

$$SDI_{a,k} = \frac{V_{a,k} - \overline{V_k}}{S_k} a = 1, 2, \ldots, k = 1, 2, 3, 4 \quad (5)$$

where S_k and $\overline{V_k}$ represent the standard deviation and the cumulative flow rate's average of the reference period and $V_{a,k}$ is a streamflow value of specified time (Nalbantis and Tsakiris 2009). The SDI criterion states that values greater than zero show wet situations, and values lower than zero indicate hydrological drought conditions according to Table 1 (Tigkas et al. 2015).

2.3 Analysis of drought trends and the relationship between hydrological and meteorological drought indices

The Spearman Rho (SRHO) and Mann–Kendall (MK) tests are used to assess trends in drought occurrences. The MK test has the advantage of assuming that the data points are independent of each other, and it doesn't require the data to follow any particular distribution (Lai et al. 2016; Wang et al. 2017). Nonparametric MK and SR have been employed extensively for time series trend analysis. According to this methodology, the test statistic S is assessed as

$$S = \sum_{k=1}^{n-1} \sum_{j=k+1}^{n} sgn(x_j - x_k) \quad (6)$$

where n denotes the number of the data, t_i is considered as the length of the tied rank group and x_j and x_k represent the data point in years j and k (j > k).

$$sgn(x_J - x_k) = \begin{cases} 1(x_j - x_k) > 0 \\ 0(x_j - x_k) = 0 \\ -1(x_j - x_k) < 0 \end{cases} \quad (7)$$

$$Var(S) = \frac{n(n-1)(2n+5) - \sum_i^r t_i(t_i - 1)(2t_i + 5)}{18} \quad (8)$$

$$Z = \begin{cases} \frac{S-1}{\sqrt{Var(S)}} S > 0 \\ 0 S = 0 \\ \frac{S+1}{\sqrt{Var(S)}} S < 0 \end{cases} \quad (9)$$

A positive Z number indicates an upward tendency, while a negative one indicates a downward trend. The statistical values for the crucial test at the 90%, 95%, and 99 percent probability levels are 1.645, 1.96, and 2.57, respectively (Yuce and Esit 2021). Like the MK test, The SRHO test, a nonparametric method, identifies monotonic trends in time series data (Yue et al. 2002). Under the H0 hypothesis, the data series is considered to be uniform, indicating the absence of any discernible trend. The following formula is used to calculate the SR correlation coefficient (r_s) and z as:

$$r_s = 1 - \frac{[6\sum_{i=1}^{n}(Rx_i - i)^2)]}{n(n^2 - 1)} \quad (10)$$

$$z = r_s \sqrt{n - 1} \quad (11)$$

Rx_i (rank statistic) is acquired through data sorting, where n is the time series' length. Positive z values show rising trends while negative z values show falling trends. (Shadmani et al. 2012).

To assess the coherence of the cross-wavelet transform between time series in a time–frequency, one can utilize wavelet transform coherence (WTC). Many areas have made substantial use of the common variation zone of two-time series in the time–frequency space (Torrence and Webster 1999). The WTC of two signals is described as follows:

$$R_n^2(s) = \frac{\left|S\left(s^{-1} W_n^{XY}(s)\right)\right|^2}{S\left(s^{-1}\left|W_n^X(s)\right|^2\right) S\left(s^{-1}\left|W_n^Y(s)\right|^2\right)} \quad (12)$$

where S is a smoothing operator and W_n^{XY} is the cross-wavelet transform defined as follows:

$$S(W) = S_{scale}\left(S_{time}(W(s))\right) \quad (13)$$

where S_{time} and S_{scale} denote smoothing along the wavelet telescopic scale axis and wavelet time translation axis, respectively. Equations (14) and (15) provide a appropriate smoothing operator for the Morlet wavelet, in which Π denotes the rectangle function, c_1, and c_2 reveal normalized constants, and the scale de-correlation length for the Morlet wavelet is established empirically to be 0.6 (Grinsted et al. 2004). The smoothing operator of a Morlet wavelet is specifically defined as:

$$S_{time}(W)|_s = \left(W_n(s) c_1^{-\frac{t^2}{2s^2}}\right)|_s \quad (14)$$

$$S_{scale}(W)|_s = \left(W_n(s) c_2 \Pi(0.6s)\right)|_s \quad (15)$$

Figure 2 explain step by step methodology flowchart for analyzing the relationship between meteorological and hydrological drought. a comprehensive methodology is analyzed to drought conditions, beginning with the collection of monthly precipitation and streamflow data for meteorological and hydrological assessments, respectively. Drought indices, including the Standardized Precipitation

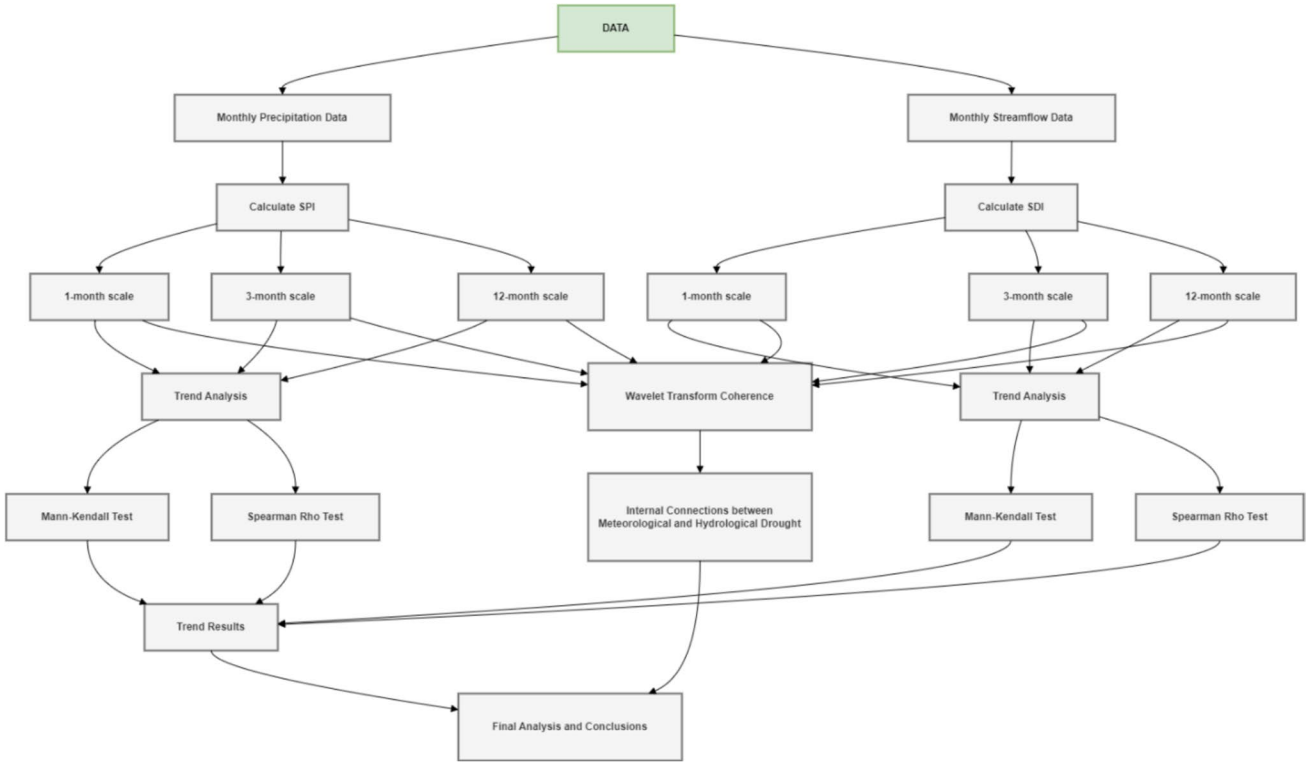

Fig. 2 The methodological Steps for Multi-Scale Drought Assessment

Index (SPI) and Streamflow Drought Index (SDI), are calculated at 1-month, 3-month, and 12-month scales to represent both meteorological and hydrological drought conditions. Trend analysis, using the Mann–Kendall and Spearman Rho tests, is then conducted to determine the presence and strength of temporal trends in these indices. Furthermore, Wavelet Transform Coherence is applied to investigate the relationship between SPI and SDI across various timescales, revealing the dynamic interplay between meteorological and hydrological drought.

3 Result and discussion

3.1 Monthly trend analysis of drought occurrences

This study investigated drought trend dynamics within the Yeşilırmak Basin by employing the non-parametric Mann–Kendall (MK) and Spearman's Rho (SRHO) tests. These statistical analyses were conducted to ascertain the presence and direction of monotonic trends in drought indices across multiple temporal scales (1-month, 3-month, and 12-month), utilizing a significance level of $\alpha = 0.05$. The tests were applied to time-series data of monthly observations for each monitoring station, facilitating the identification of statistically significant temporal variations. An increasing trend in SPI/SDI values indicates an absence of drought, while a decreasing trend suggests drought conditions. Figures 3 and 4 depict the monthly trends for hydrological and meteorological droughts, respectively, across all timescales. For the SPI 1-month timescale, a significant decreasing trend is observed in February for station 17030. Conversely, significant increasing trends are found in June for station 17082, and in April and December for station 17083, as well as May for station 17083 (based on both trend tests). On the SPI 3-month timescale, stations 17030 and 17712 show decreasing trends in April and June, respectively. In contrast, station 17083 exhibits increasing trends in all months except February, March, and July. An increasing trend of SPI values is observed in June and July for station 17082, July for station 17085, and October and December for stations 17140 and 17681. Trend analysis of the 12-month SPI, using MK and SRHO tests, revealed no significant decreasing trends, indicating no widespread intensification of meteorological drought. However, stations 17083, 17084, and 17140 consistently exhibited significant increasing trends across all months, signifying a consistent absence of substantial drought conditions at these locations over the extended timescale.

Analysis of the 1-month SPI revealed varying trends across different stations in the basin. Five stations (D14A011, D14A014, E14A022, E14A028, and E14A032)

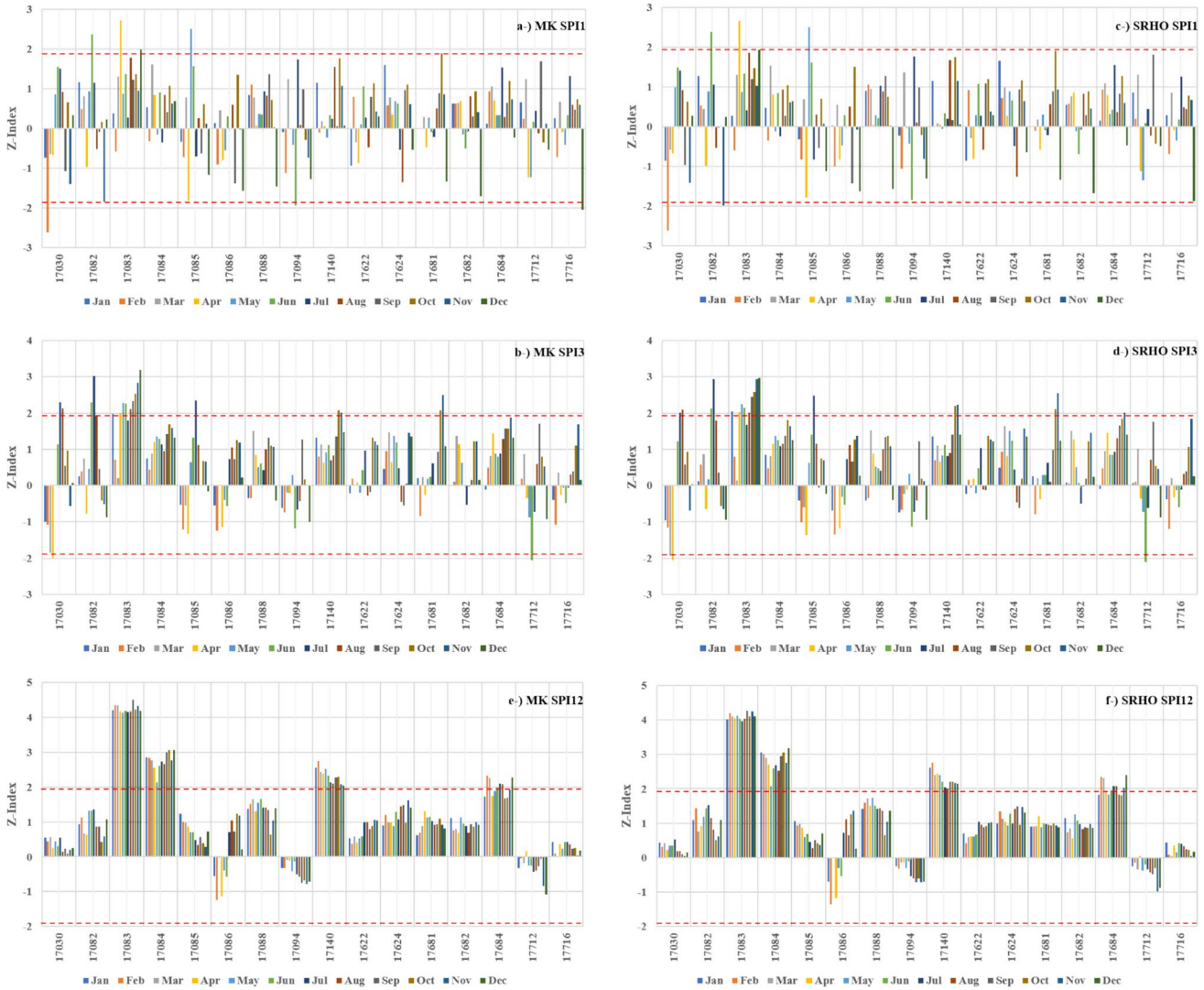

Fig. 3 The monthly trend analysis of meteorological stations used in the study by MK and SRHO tests at 1-, 3- and 12-month time scales

showed no statistically significant trends. However, three stations exhibited positive trends: D14A126 showed increasing trends in June, D14A127 in May, and E14A001 demonstrated increasing trends during January and July through December. Several stations displayed negative trends: D14A119 showed decreasing trends in January and October through December; D14A126 in January through March and November through December; D14A127 in November and December; D14A133 in April and October through December; E14A001 in March through May; E14A018 in August and September; and E14A030 in November."Overall, a significant trend (at the 5% level) was identified at many hydrological stations. The findings for the 3-month SPI timescale mirrored those of the 1-month timescale. For the 12-month SPI timescale, most stations showed no significant trends, with exceptions at D14A119 (January, February, and September-December) and E14A001 (March-July).

3.2 Comparison between meteorological and hydrological drought

To understand the relation between these two types of droughts, a comparative analysis is conducted. Data from precipitation and streamflow stations located in close proximity to each other were used in the analysis. Figure 5 illustrates the station pairs considered for the study area, including D14A014-17030, D14A119-17681, D14A133-17085, E14A001-17086, E14A018-17086, E14A022-17088, and E14A022-17094. To ensure a robust comparison, drought indices (SDI and SPI) were overlaid for the same hydrological year.

Analyzing the relationship between station D14A014 and 17030, we observe the most severe meteorological droughts (based on SPI values) occurring in the years 1964, 1971, 1984, 1986, 1996, 1997, 2000, 2014, and 2018. However,

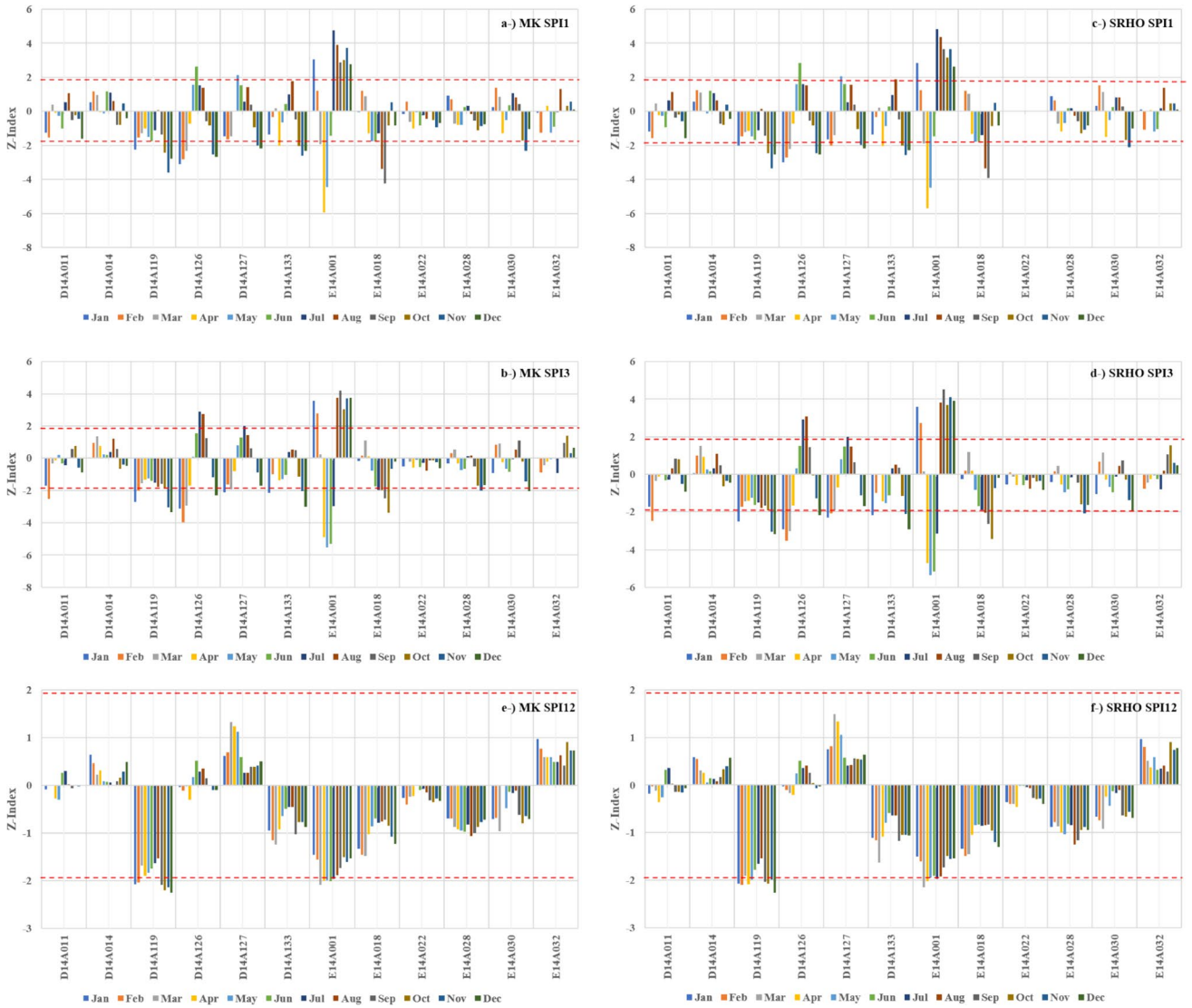

Fig. 4 The monthly trend analysis of hydrological stations used in the study by MK and SRHO tests at 1-, 3- and 12-month time scales

the 1-month SDI identified 1996 as the sole hydrological drought year within the study period. Conversely, the Standardized Precipitation Index (SPI) indicated 1986 as the year of most severe meteorological drought, with a minimum value of −3.58. Furthermore, a temporal discrepancy was observed between hydrological and meteorological drought indicators; the 12-month SDI reached its maximum value between October 1997 and May 1998, a period during which the SPI values generally reflected normal conditions." However, both SPI and SDI indices consistently identify 2014 as an extreme drought year at both 3-month and 12-month timescales. Moving on to stations D14A119 and 17681, SPI values at the 1-month timescale capture the most significant drought event. Here, both indices agree that 2001 experienced the most extreme events, with droughts occurring at the 3-month and 12-month timescales, respectively.

Figure 6 highlights the most extreme events identified by both SPI and SDI indices using red boxes. Analysis of extreme drought frequencies at the 1-month timescale revealed a tendency for meteorological stations to register a higher incidence of extreme drought events compared to hydrological stations. However, this discrepancy diminished at the 3-month and 12-month timescales, where concurrence between meteorological and hydrological drought index classifications increased. Notably, hydrological stations E14A018 and E14A022 exhibited a unique pattern, consistently indicating extreme drought conditions throughout 2014 across all temporal scales, despite corresponding meteorological stations classifying this period as one of normal drought severity. This suggests that long-term trends (3-month and 12-month) may be more reliable indicators of drought in these specific locations compared

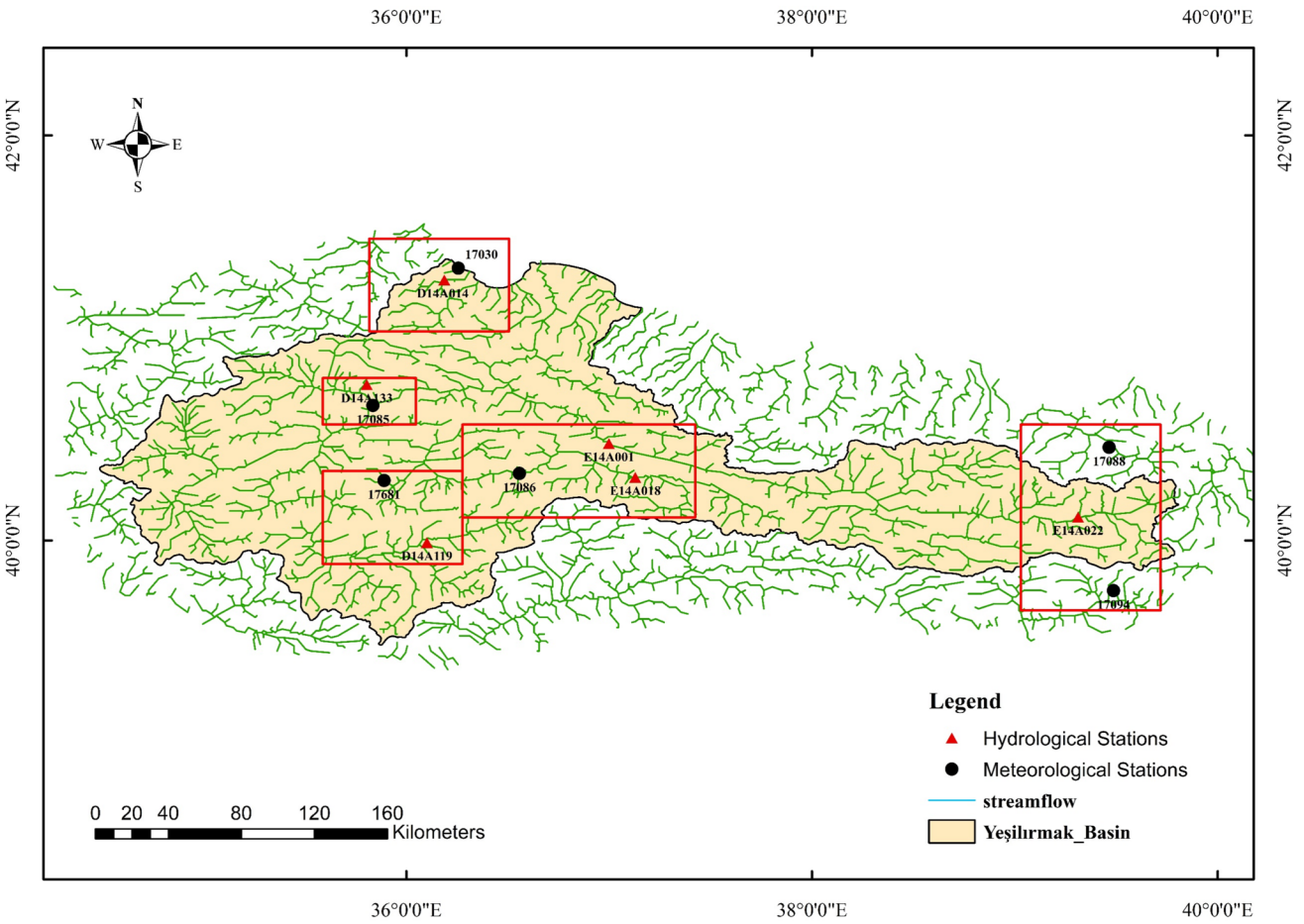

Fig. 5 The geographical positions of the chosen meteorological and hydrological stations employed in the research

to short-term (1-month) variations. Our findings are convenient with previous studies (Boudad et al. 2018; Wu et al. 2018).

Figure 7 presents heat maps for the selected stations, depicting long-term meteorological and hydrological droughts based on both SPI and SDI indices. These drought heat maps visually represent the temporal trends in drought duration and severity over time. They are valuable tools for analyzing the timing, location, severity, and duration of droughts. Additionally, they allow for a comparative analysis of drought characteristics across different meteorological and hydrological stations. In Fig. 6, blue and red colors represent dry and wet periods, respectively. Stations D14A014 and D14A119 exhibit more frequent droughts compared to other stations at the 1-month and 3-month timescales. However, all stations show a good agreement on drought patterns at the 12-month timescale.

Spearman's rank correlation analysis, as presented in Table 2, demonstrates a positive relationship between the SPI and SDI across all monitoring stations. Notably, the strength of this correlation exhibited a direct relationship with the temporal scale, with the 12-month timescale showing the highest correlation, followed by the 3-month and 1-month timescales. The maximum correlation coefficient of 0.58 was observed between SPI and SDI at stations D14A119 and 17681 for the 12-month timescale, whereas the minimum correlation of 0.14 was found at stations E14A001 and 17086. Moreover, the correlation coefficient increased with increasing time lag between the indices. These results indicate that SPI and SDI provide complementary information and can be effectively utilized in conjunction for comprehensive drought monitoring across varying temporal scales. For instance, the strong correlation at longer timescales (12-month) makes them suitable for monitoring reservoir storage, while the positive correlation at shorter timescales (1-month) indicates their potential for monitoring streamflow and groundwater levels. This paper's results have good agreement with previous studies by Abro et al., (2022) and Salimi et al., (2021).

This section evaluates the correlations between the monthly SDI and SPI drought indices in the study area using WTC analysis. WTC is utilized to determine if there exists a notable oscillatory period among the selected drought

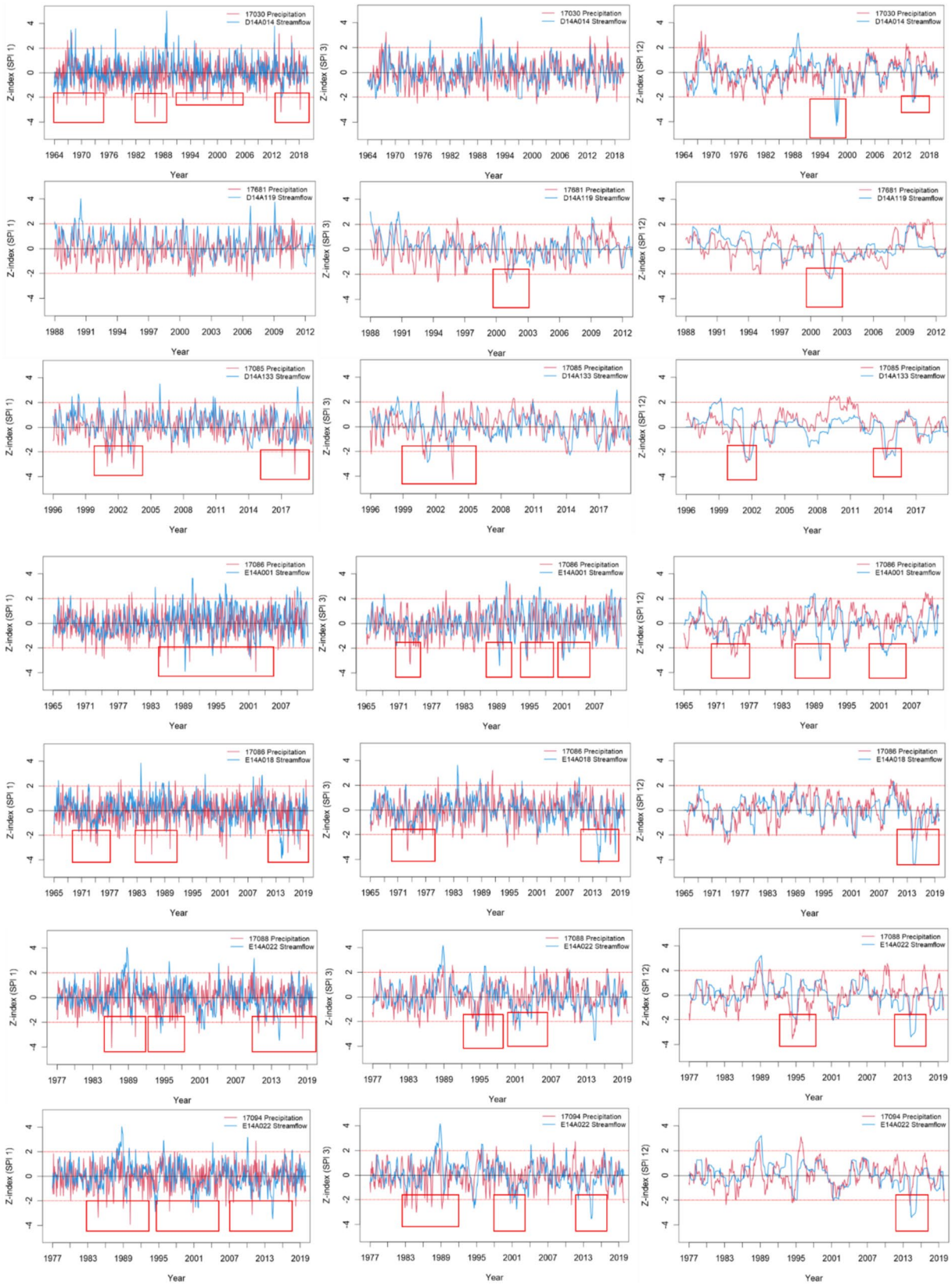

Fig. 6 The major drought occurrences using SPI/SDI drought indices for selected stations

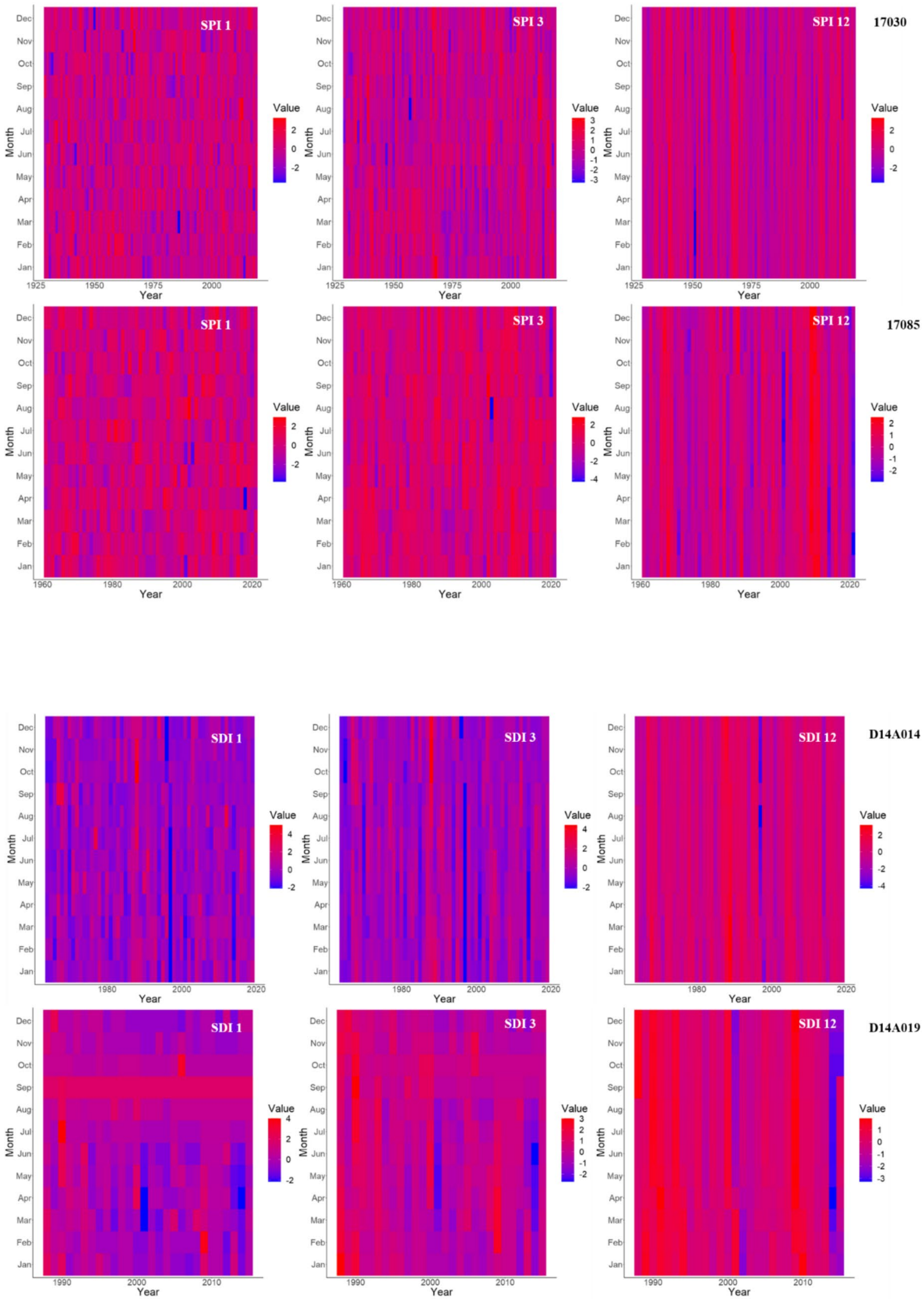

Fig. 7 Meteorological and hydrological drought heat map of SPI/SDI 1-, 3- and 12-month time scale for selected stations (stations 17030, 17085, D14A014, and D14A019)

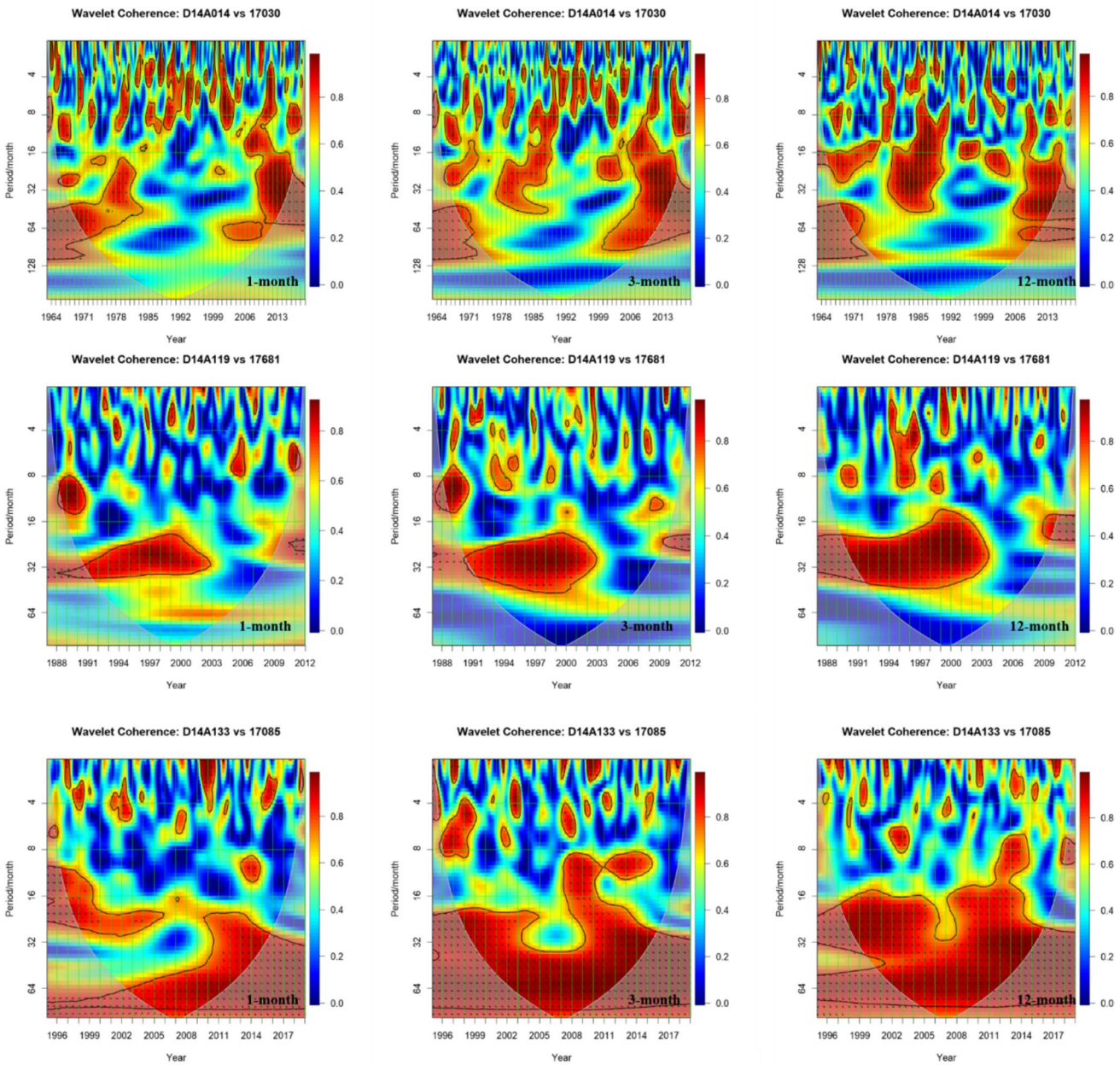

Fig. 8 The monthly SPI and SDI drought indices at various time scales are compared using WTC analysis. The thick enclosed portions in the figures indicate a statistical significance level of 5% compared to a red noise process, and the arrows show the phase difference of periods and coherence of more than 0.5 between the two data series

indices. Figure 8 illustrates the results of the WTC analysis depicting the relationships among the drought indices across various time scales (1-, 3-, and 12-month). To demonstrate the cause-and-effect relationships between the utilized indices, each panel in this figure displays a relative phasing of the two-time series. In the colder regions beyond the main areas (depicted by bluish regions), frequencies and timings showed no dependency on time. The phase patterns serve to assess the causality relationship between the two-time series. When arrow directions move to the right, hydrological and meteorological stations are in phase, or favorably coupled. This is the meaning of the arrow direction. Arrows pointing in various directions show lags or leads between two-time series. Arrow orientations shifting to the left indicate that hydrological and meteorological stations are in anti-phase (negatively related). For example, the hydrological station's leadership is shown by arrows pointing left or up, whereas the meteorological station's leadership is indicated by arrows

pointing left or up. The meteorological and hydrological stations are represented by the first and second variables in Fig. 7, respectively.

Only major portions of the WTC graph should be considered to get the most accurate understanding. From the results, the WTC provided by the D14A014-17030 reveals significant positive period signals of the 16–65 months during 1968–1984, 3–64 months in 2006–2016, and the low band has a positive signal of 0–12 months observed for 1-month time scale. The primary major positive period signals, when taking into account the 3- and 12-month time scales, are 6–48 months from 1977 to 1990, 16–30 months from 1999 to 2004, and 6–60 months from 2006 to 2016. There is a good correlation between stations D14A119 and 17681. For all time scales, the signal's major positive period was primarily concentrated in the cycle of 18–35 months from 1991–2003, and 8–15 months from 1988–1991 for 1- and 3-month time scales. At all time scales, no anti-phase links are detected.

WTC analysis of stations D14A133 and 17085 reveals a strong positive correlation within the 8–32 month band from 1996 to 2005. Additionally, positive period signals are observed at the 1-month timescale within the 16–64 month band, ranging from 2002 to 2016. Furthermore, WTC analysis indicates an in-phase relationship between hydrological and meteorological droughts at the 3- and 12-month timescales within the 8–64 month band, from 1997 to 2016. Wavelet Transform Coherence (WTC) offers valuable insights into the internal relationship between hydrological and meteorological droughts within the Yeşilırmak basin. It effectively reveals the connections and unique characteristics of how these droughts' oscillation periods change over time. WTC analysis suggests a slight time lag between the occurrences of hydrological and meteorological droughts, with a positive correlation between the two. This indicates that a hydrological drought may precede the onset of a meteorological drought. Notably, for most stations, the positive correlation between the monthly signals is statistically significant at the 3-month and 12-month timescales, but not as significant at the 1-month timescale.

4 Conclusions

This study investigated meteorological and hydrological droughts in the Yeşilırmak Basin using the Standardized Precipitation Index (SPI) and the Standardized Streamflow Index (SDI), respectively, across multiple timescales. Our key findings are:

- Timescale-Dependent Drought Trends: While some significant short-term (1- and 3-month) drought trends were identified for both meteorological and hydrological droughts at individual stations, no significant long-term (12-month) trends were observed basin-wide. This highlights the importance of considering multiple timescales in drought analysis. According to Abro et al. (2022) and Esit et al. (2023b), Several drought indices are capable of capturing major droughts in the basin, particularly those lasting 12 months or longer. Our findings are further corroborated by existing literature (Wubneh et al. 2023; Fowé et al. 2023; Wang et al. 2024)
- Discrepancies and Agreement between SPI and SDI: At the 1-month timescale, meteorological droughts (SPI) were often more severe than hydrological droughts (SDI). However, at longer timescales (3 and 12 months), SPI and SDI showed increasing agreement in identifying drought events, indicating a stronger connection between accumulated meteorological deficits and hydrological drought. Notably, some hydrological stations experienced persistent drought conditions even when corresponding meteorological data indicated normal conditions, suggesting the influence of other factors on hydrological drought. Our study supports the findings of previous research (Kubiak-Wójcicka et al. 2021)
- Strengthening Correlation at Longer Timescales: The correlation between SPI and SDI strengthened considerably at the 12-month timescale compared to the 1-month timescale, suggesting that long-term precipitation deficits are more reliably reflected in streamflow reductions. This was further supported by wavelet coherence analysis, which revealed a stronger positive association between SPI and SDI at longer timescales.

These findings demonstrate the effectiveness of SPI and SDI, particularly at longer timescales, for capturing major drought events in the Yeşilırmak Basin. The stronger correlation between SPI and SDI at longer timescales provides valuable insights for water resource management. Specifically, the observed link between long-term meteorological deficits and hydrological drought can inform the development of proactive water management strategies, such as implementing water conservation measures during periods of projected SPI decrease. While this study focused on meteorological and hydrological droughts within a single basin, future research could expand the scope to include other drought types, a wider geographical area, and longer time series, as well as investigate the underlying causes of the identified drought events. This will further enhance our understanding of drought dynamics and inform more robust mitigation and adaptation strategies in the face of potential future climate change impacts.

Acknowledgements The State Water Works (DSI) and the General Directorate of Meteorology (MGM) are to be acknowledged for their contributions of meteorological data.

Author contribution M.I.Yuce and A. Aytek: Revised manuscript, M. Esit: Provided data and write manuscript, İ. H. Deger, F. Uğur and A. Simsek: Observed analysis.

Funding Not applicable.

Data availability No datasets were generated or analysed during the current study.

Declarations

Ethics approvals Not applicable.

Consent to participate Not applicable.

Consent for publication Not applicable.

Competing interest The authors declare no competing interests.

Code availability Not applicable.

Informed consent This study did not include any human participants or animals.

References

Abbas S, Kousar S (2021) Spatial analysis of drought severity and magnitude using the standardized precipitation index and streamflow drought index over the Upper Indus Basin, Pakistan. Environ Dev Sustain 23:15314–15340. https://doi.org/10.1007/s10668-021-01299-y

Abbas A, Waseem M, Ullah W et al (2021) Spatiotemporal analysis of meteorological and hydrological droughts and their propagations. Water 13:2237. https://doi.org/10.3390/w13162237

Abeysingha NS, Wickramasuriya MG, Meegastenna TJ (2020) Assessment of meteorological and hydrological drought; a case study in Kirindi Oya river basin in Sri Lanka. Int J Hydrol Sci Technol 10:429–447. https://doi.org/10.1504/IJHST.2020.109947

Abro MI, Elahi E, Chand R et al (2022) Estimation of a trend of meteorological and hydrological drought over Qinhuai River Basin. Theor Appl Climatol 147:1065–1078. https://doi.org/10.1007/s00704-021-03870-z

AghaKouchak A, Farahmand A, Melton FS et al (2015) Remote sensing of drought: Progress, challenges and opportunities. Rev Geophys 53:452–480. https://doi.org/10.1002/2014RG000456

Aghelpour P, Bahrami-Pichaghchi H, Varshavian V (2021) Hydrological drought forecasting using multi-scalar streamflow drought index, stochastic models and machine learning approaches, in northern Iran. Stoch Environ Res Risk Assess 35:1615–1635. https://doi.org/10.1007/s00477-020-01949-z

Ahmadalipour A, Moradkhani H, Demirel MC (2017) A comparative assessment of projected meteorological and hydrological droughts: Elucidating the role of temperature. J Hydrol 553:785–797. https://doi.org/10.1016/j.jhydrol.2017.08.047

Akbari H, Rakhshandehroo GR, Sharifloo AH, Ostadzadeh E (2015) Drought Analysis Based on Standardized Precipitation Index (SPI) and Streamflow Drought Index (SDI) in Chenar Rahdar River Basin, Southern Iran. 11–22. https://doi.org/10.1061/9780784479322.002

Alley WM (1984) The palmer drought severity index: limitations and assumptions. J Appl Meteorol Climatol 23:1100–1109. https://doi.org/10.1175/1520-0450(1984)023%3c1100:TPDSIL%3e2.0.CO;2

Anshuka A, van Ogtrop FF, Willem Vervoort R (2019) Drought forecasting through statistical models using standardised precipitation index: a systematic review and meta-regression analysis. Nat Hazards 97:955–977. https://doi.org/10.1007/s11069-019-03665-6

Boudad B, Sahbi H, Mansouri I (2018) Analysis of meteorological and hydrological drought based in SPI and SDI index in the Inaouen Basin (Northern Morocco). J Mater Environ Sci 9(1):219–27. https://doi.org/10.26872/jmes.2018.9.1.25

Boustani A, Ulke A (2020) Investigation of meteorological drought indices for environmental assessment of Yesilirmak Region. J Environ Treat Tech 8(1):374–381

Cemek B, Demir Y, Güler M, Karaman S (2007) THE EVALUATION OF DIFFERENT ARID CONDITIONS USING GEOGRAPHIC INFORMATION SYSTEMS IN YESILIRMAK BASIN. InProceed IntCongress River Basin Manag 2:68–77

Cheraghalizadeh M, Ghameshlou AN, Bazrafshan J, Bazrafshan O (2018) A copula-based joint meteorological–hydrological drought index in a humid region (Kasilian basin, North Iran). Arab J Geosci 11:300. https://doi.org/10.1007/s12517-018-3671-7

Esit M, Çelik R, Akbas E (2023a) Spatial and temporal variation of meteorological parameters in the lower Tigris-Euphrates basin, Türkiye: application of non-parametric methods and an innovative trend approach. Water Sci Technol 87:1982–2004. https://doi.org/10.2166/wst.2023.116

Esit M, Çelik R, Akbas E (2023b) Long-term meteorological and hydrological drought characteristics on the lower Tigris-Euphrates basin, Türkiye: relation, impact and trend. Environ Earth Sci 82:491. https://doi.org/10.1007/s12665-023-11182-w

Esit M, Kumar S, Pandey A et al (2021) Seasonal to multi-year soil moisture drought forecasting. npj Clim Atmos Sci 4(1):16. https://doi.org/10.1038/s41612-021-00172-z

Fowé T, Yonaba R, Mounirou LA et al (2023) From meteorological to hydrological drought: a case study using standardized indices in the Nakanbe River Basin, Burkina Faso. Nat Hazards 119:1941–1965. https://doi.org/10.1007/s11069-023-06194-5

Ganguli P, Singh B, Reddy NN et al (2022) Climate-catchment-soil control on hydrological droughts in peninsular India. Sci Rep 12:8014. https://doi.org/10.1038/s41598-022-11293-7

Grinsted A, Moore JC, Jevrejeva S (2004) Application of the cross wavelet transform and wavelet coherence to geophysical time series. Nonlinear Process Geophys 11:561–566. https://doi.org/10.5194/npg-11-561-2004

Jamal M, Ebrahimi H, Jahromi HM (2022) Effect of selecting the superior probability distribution in modifying streamflow drought index (SDI). Arab J Geosci 15:785. https://doi.org/10.1007/s12517-022-09970-y

Katipoğlu OM, Yeşilyurt SN, Dalkılıç HY (2022) Yeşilırmak havzasındaki hidrolojik kuraklıkların Mann-Kendall ve Yenilikçi Şen yöntemi ile trend analizi. Gümüşhane Üniversitesi Fen Bilimleri Dergisi. 12(2):422–42. https://doi.org/10.17714/gumusfenbil.1026893

Kubiak-Wójcicka K, Pilarska A, Kamiński D (2021) The analysis of long-term trends in the meteorological and hydrological drought occurrences using non-parametric methods—case study of the catchment of the upper noteć river (Central Poland). Atmosphere 12:1098. https://doi.org/10.3390/atmos12091098

Lai C, Chen X, Wang Z et al (2016) Spatio-temporal variation in rainfall erosivity during 1960–2012 in the Pearl River Basin, China. CATENA 137:382–391. https://doi.org/10.1016/j.catena.2015.10.008

Lai C, Zhong R, Wang Z et al (2019) Monitoring hydrological drought using long-term satellite-based precipitation data. Sci Total Environ 649:1198–1208. https://doi.org/10.1016/j.scitotenv.2018.08.245

Madadgar S, Moradkhani H (2014) Spatio-temporal drought forecasting within Bayesian networks. J Hydrol 512:134–146. https://doi.org/10.1016/j.jhydrol.2014.02.039

Malik A, Kumar A, Singh RP (2019) Application of Heuristic Approaches for Prediction of Hydrological Drought Using Multiscalar Streamflow Drought Index. Water Resour Manage 33:3985–4006. https://doi.org/10.1007/s11269-019-02350-4

Malik A, Kumar A, Salih SQ, Yaseen ZM (2021) Hydrological Drought Investigation Using Streamflow Drought Index. In: Deo RC, Samui P, Kisi O, Yaseen ZM (eds) Intelligent Data Analytics for Decision-Support Systems in Hazard Mitigation: Theory and Practice of Hazard Mitigation. Springer, Singapore, pp 63–88

McKee TB, Doesken NJ, Kleist J (1993) The Relationship of Drought Frequency and Duration to Time Scales. Boston, MA: Am Meteorol Soc 17:179–183

Meresa H, Murphy C, Donegan SE (2023) Propagation and Characteristics of Hydrometeorological Drought Under Changing Climate in Irish Catchments. J Geophys Res: Atmosp 128(10):22. https://doi.org/10.1029/2022JD038025

Mishra V, Cherkauer KA, Shukla S (2010) Assessment of drought due to historic climate variability and projected future climate change in the Midwestern United States. J Hydrometeorol 11:46–68. https://doi.org/10.1175/2009JHM1156.1

Nalbantis I (2008) Evaluation of a Hydrological Drought Index. Eur Water 23(24):67–77

Nalbantis I, Tsakiris G (2009) Assessment of hydrological drought revisited. Water Resour Manage 23:881–897. https://doi.org/10.1007/s11269-008-9305-1

Palmer WC (1965) Meteorological Drought US. Weather Bureau. Res Paper 45:1–58

Pei Z, Fang S, Wang L, Yang W (2020) Comparative Analysis of Drought Indicated by the SPI and SPEI at Various Timescales in Inner Mongolia. China Water 12:1925. https://doi.org/10.3390/w12071925

Peña-Gallardo M, Vicente-Serrano SM, Hannaford J et al (2019) Complex influences of meteorological drought time-scales on hydrological droughts in natural basins of the contiguous Unites States. J Hydrol 568:611–625. https://doi.org/10.1016/j.jhydrol.2018.11.026

Rivera JA, Penalba OC, Villalba R, Araneo DC (2017) Spatio-Temporal Patterns of the 2010–2015 Extreme Hydrological Drought across the Central Andes. Argentina Water 9:652. https://doi.org/10.3390/w9090652

Salimi H, Asadi E, Darbandi S (2021) Meteorological and hydrological drought monitoring using several drought indices. Appl Water Sci 11:11. https://doi.org/10.1007/s13201-020-01345-6

Satoh Y, Yoshimura K, Pokhrel Y et al (2022) The timing of unprecedented hydrological drought under climate change. Nat Commun 13:3287. https://doi.org/10.1038/s41467-022-30729-2

Sattar MN, Lee J-Y, Shin J-Y, Kim T-W (2019) Probabilistic Characteristics of drought propagation from meteorological to hydrological drought in South Korea. Water Resour Manage 33:2439–2452. https://doi.org/10.1007/s11269-019-02278-9

Shadmani M, Marofi S, Roknian M (2012) Trend Analysis in Reference Evapotranspiration Using Mann-Kendall and Spearman's Rho Tests in Arid Regions of Iran. Water Resour Manage 26:211–224. https://doi.org/10.1007/s11269-011-9913-z

Shukla S, Wood AW. Use of a standardized runoff index for characterizing hydrologic drought. Geophysical research letters. 2008 Jan;35(2). https://doi.org/10.1029/2007GL032487

Simsek O (2021) Hydrological drought analysis of Mediterranean basins. Turkey Arab J Geosci 14:2136. https://doi.org/10.1007/s12517-021-08501-5

Tabari H, Grismer ME, Trajkovic S (2013) Comparative analysis of 31 reference evapotranspiration methods under humid conditions. Irrig Sci 31:107–117. https://doi.org/10.1007/s00271-011-0295-z

Tigkas D, Vangelis H, Tsakiris G (2015) DrinC: a software for drought analysis based on drought indices. Earth Sci Inform 8:697–709. https://doi.org/10.1007/s12145-014-0178-y

Tijdeman E, Barker LJ, Svoboda MD, Stahl K (2018) Natural and human influences on the link between meteorological and hydrological drought indices for a large set of catchments in the Contiguous United States. Water Resour Res 54:6005–6023. https://doi.org/10.1029/2017WR022412

Tokarczyk T, Szalińska W (2014) Combined analysis of precipitation and water deficit for drought hazard assessment. Hydrol Sci J 59:1675–1689. https://doi.org/10.1080/02626667.2013.862335

Torrence C, Webster PJ (1999) Interdecadal Changes in the ENSO–Monsoon System. J Clim 12:2679–2690. https://doi.org/10.1175/1520-0442(1999)012%3c2679:ICITEM%3e2.0.CO;2

Vicente-Serrano SM, Beguería S, López-Moreno JI (2010) A Multiscalar Drought Index Sensitive to Global Warming: The Standardized Precipitation Evapotranspiration Index. J Climate 23:1696–1718. https://doi.org/10.1175/2009JCLI2909.1

Vicente-Serrano SM, López-Moreno JI, Santiago B et al (2012a) Accurate Computation of a Streamflow Drought Index. J Hydrol Eng 17:318–332. https://doi.org/10.1061/(ASCE)HE.1943-5584.0000433

Vicente-Serrano SM, Beguería S, Lorenzo-Lacruz J et al (2012b) Performance of Drought Indices for Ecological, Agricultural, and Hydrological Applications. Earth Interact 16:1–27. https://doi.org/10.1175/2012EI000434.1

Wang H, Pan Y, Chen Y (2017) Comparison of three drought indices and their evolutionary characteristics in the arid region of northwestern China. Atmosp Sci Letters 18:132–139. https://doi.org/10.1002/asl.735

Wang Y, Zhang T, Chen X et al (2018) Spatial and temporal characteristics of droughts in Luanhe River basin, China. Theor Appl Climatol 131:1369–1385. https://doi.org/10.1007/s00704-017-2059-z

Wang Z, Chang J, Wang Y et al (2024) Temporal and spatial propagation characteristics of meteorological drought to hydrological drought and influencing factors. Atmos Res 299:107212. https://doi.org/10.1016/j.atmosres.2023.107212

WMO (2006) Drought Monitoring and Early Warning: Concepts, Progress, and Future Challenges. In: World Meteorological Organization. https://public.wmo.int/en/resources/library/drought-monitoring-and-early-warning-concepts-progress-and-future-challenges. Accessed 23 Feb 2020

Wu J, Chen X, Gao L et al (2016) Response of Hydrological Drought to Meteorological Drought under the Influence of Large Reservoir. Advances in Meteorology 2016:e2197142. https://doi.org/10.1155/2016/2197142

Wu J, Liu Z, Yao H et al (2018) Impacts of reservoir operations on multi-scale correlations between hydrological drought and meteorological drought. J Hydrol 563:726–736. https://doi.org/10.1016/j.jhydrol.2018.06.053

Wubneh MA, Alemu MG, Fekadie FT et al (2023) Meteorological and hydrological drought monitoring and trend analysis for selected gauged watersheds in the Lake Tana basin, Ethiopia: Under future climate change impact scenario. Scientif African 20:e01738. https://doi.org/10.1016/j.sciaf.2023.e01738

Xu Z, Wu Z, He H et al (2019) Evaluating the accuracy of MSWEP V2.1 and its performance for drought monitoring over mainland China. Atmos Res 226:17–31. https://doi.org/10.1016/j.atmosres.2019.04.008

Yalçın S, Eşit M, Çoban Ö (2023) A new deep learning method for meteorological drought estimation based-on standard precipitation evapotranspiration index. Eng Appl Artif Intell 124:106550. https://doi.org/10.1016/j.engappai.2023.106550

Yaşa İ, Partal T (2024) Drought trend and variability based wavelet transform in Euphrates-Tigris Basin. Türkiye Atmospheric Research 302:107291. https://doi.org/10.1016/j.atmosres.2024.107291

Yildirim I, Aksoy H (2022) Intermittency as an indicator of drought in streamflow and groundwater. Hydrol Process 36:e14615. https://doi.org/10.1002/hyp.14615

Yuce MI, Esit M (2021) Drought monitoring in Ceyhan Basin, Turkey. J Appl Water Eng Res 9:293–314. https://doi.org/10.1080/23249676.2021.1932616

Yue S, Pilon P, Cavadias G (2002) Power of the Mann-Kendall and Spearman's rho tests for detecting monotonic trends in hydrological series. J Hydrol 259:254–271. https://doi.org/10.1016/S0022-1694(01)00594-7

Zambrano F, Wardlow B, Tadesse T et al (2017) Evaluating satellite-derived long-term historical precipitation datasets for drought monitoring in Chile. Atmos Res 186:26–42. https://doi.org/10.1016/j.atmosres.2016.11.006